

Overview of Polarimetry



Ken Moffeit, *SLAC*

2009 Linear Collider Workshop of the Americas
29 September to 3 October 2009

Outline of Talk

Polarized Physics

Machine-Detector Interface Issues

Upstream Polarimeter

Downstream Polarimeter

Polarimetry at CLIC

Physics with polarized beams

'Scope Document no.1' (2003) and 'no.2' (2006): baseline

'full luminosity of $2 \times 10^{34} \text{ cm}^2\text{s}^{-1}$ '

'electron beams with polarisation >80% within whole energy range.'

Options:

'e+ polarisation ~50% in whole energy range wo sign. loss of lumi....,

Reversal of helicity ... between bunch crossings.'

GigaZ: e+ polarisation+frequent flips essential.'

$$\sigma_{P_{e^-}P_{e^+}} = \frac{1}{4} \left\{ (1 + P_{e^-})(1 + P_{e^+})\sigma_{RR} + (1 - P_{e^-})(1 - P_{e^+})\sigma_{LL} \right. \\ \left. + (1 + P_{e^-})(1 - P_{e^+})\sigma_{RL} + (1 - P_{e^-})(1 + P_{e^+})\sigma_{LR} \right\}$$

σ_{RL} e- beam is completely right-handed polarized ($P_{e^-} = +1$)
e+ beam is completely left-handed polarized ($P_{e^+} = -1$)

	e^-	e^+		
σ_{RR}			$\frac{1+P_{e^-}}{2} \cdot \frac{1+P_{e^+}}{2}$	$J_z = 0$
σ_{LL}			$\frac{1-P_{e^-}}{2} \cdot \frac{1-P_{e^+}}{2}$	
σ_{RL}			$\frac{1+P_{e^-}}{2} \cdot \frac{1-P_{e^+}}{2}$	$J_z = 1$
σ_{LR}			$\frac{1-P_{e^-}}{2} \cdot \frac{1+P_{e^+}}{2}$	

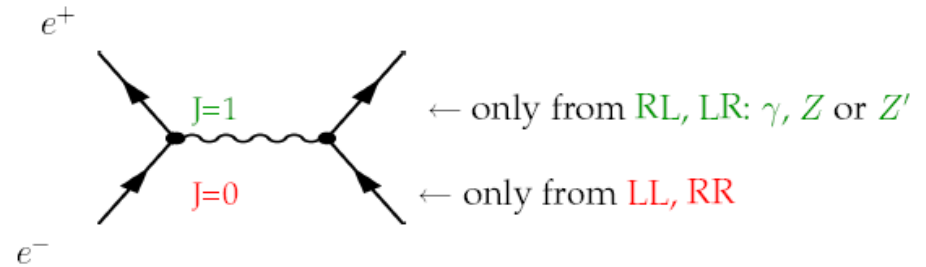
Physics with polarized beams: motivation and requirements

Standard Model only $J = 1$ is possible.

New Physics models:

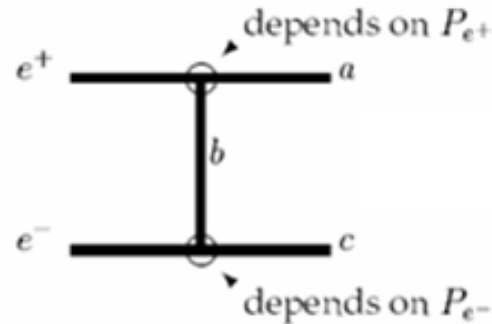
may contribute to $J = 1$

may allow the production of scalar particles,
 $J = 0$ would be allowed



Exchange Diagrams

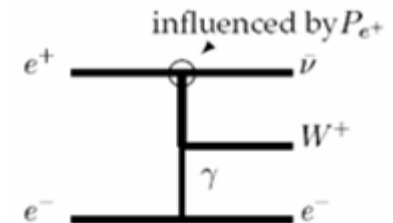
Helicity of e^- not coupled with helicity of e^+



T - and U - channel diagrams

The helicity of the incoming beam is directly coupled to the helicity of the final particle and is completely independent of the helicity of the second incoming particle.

Single W^+ production: the vertex $e^+W^+\nu$ depends only on P_{e^+} .



Physics with polarized beams

Cross section enhanced or reduced

The cross sections can be enhanced or reduced by an appropriate choice of the polarization states. This allows to suppress the background: For instance, a ratio of 'undesired' to 'desired' polarization states, $[(1 - P_{e^-})(1 - P_+)]/[(1 + P_{e^-})(1 + P_{e^+})]$, yields a background reduction by a factor 4 having (80%, 60%) polarization instead of (80%, 0%). A positron polarisation of 30% reduces this undesired background by a factor 2.

Positron Polarization important

Comparison with ($P_{e^-} = 80\%$, $P_{e^+} = 0\%$) estimated gain factor when ($P_{e^-} = 80\%$, $P_{e^+} = 60\%$) ($P_{e^-} = 80\%$, $P_{e^+} = 30\%$)

Case	Effects for $P(e^-) \rightarrow P(e^-)$ and $P(e^+)$	Gain & Requirement	
Standard Model:			$P_{e^-}^T P_{e^+}^T$ required
top threshold	Electroweak coupling measurement	factor 3	gain factor 2
$t\bar{q}$	Limits for FCN top couplings improved	factor 1.8	gain factor 1.4
CPV in $t\bar{t}$	Azimuthal CP-odd asymmetries give access to S- and T-currents up to 10 TeV	$P_{e^-}^T P_{e^+}^T$ required	$P_{e^-}^T P_{e^+}^T$ required
W^+W^-	Enhancement of $\frac{S}{B}, \frac{S}{\sqrt{B}}$	up to a factor 2	
	TGC: error reduction of $\Delta\kappa_\gamma, \Delta\lambda_\gamma, \Delta\kappa_Z, \Delta\lambda_Z$	factor 1.8	
	Specific TGC $\tilde{h}_+ = \text{Im}(g_1^R + \kappa^R)/\sqrt{2}$	$P_{e^-}^T P_{e^+}^T$ required	
CPV in γZ	Anomalous TGC $\gamma\gamma Z, \gamma Z Z$	$P_{e^-}^T P_{e^+}^T$ required	
HZ	Separation: $HZ \leftrightarrow H\nu\nu$	factor 4	gain factor 2
	Suppression of $B = W^+ \ell^- \nu$	factor 1.7	
$t\bar{t}H$	Top Yukawa coupling measurement at $\sqrt{s} = 500$ GeV	factor 2.5	gain factor 1.6

Machine-Detector Interface Issues

BDS and Polarimeter Alignment

Accelerator Alignment Tolerances (from RDR Volume 3, Table 4.7-1)

Area	Type	Tolerance
Sources, Damping Rings and RTML	Offset	150 μm (horizontal and vertical), over a distance of 100 m.
	Roll	100 μrad
Main Linac (cryomodules)	Offset	200 μm (horizontal and vertical), over a distance of 200 m.
	Pitch	20 μrad
	Roll	
BDS	Offset	150 μm (horizontal and vertical), over a distance of 150 m around the IR.

- locally, achieve 1 μrad over distances up to 200m
- can probably extrapolate this to achieving 10 μrad over 2000m; will be complicated by the 1.5m offset of the upstream polarimeter IP
→ need to flesh out procedure

Spin precession:

$$\theta_{spin} = \gamma \frac{g-2}{2} \cdot \theta_{bend} = \frac{E(\text{GeV})}{0.44065} \cdot \theta_{bend}$$

at E = 250 GeV,

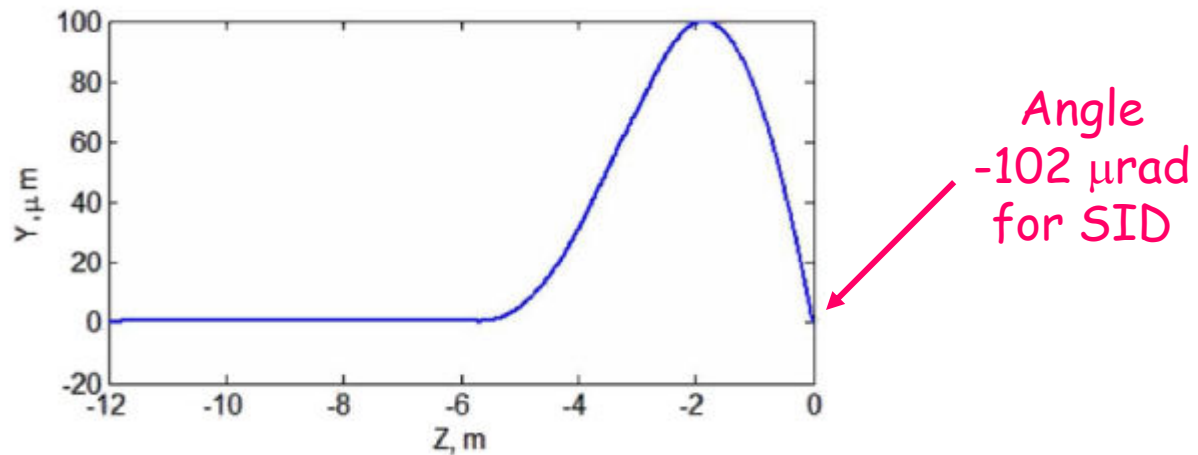
θ_{bend}	θ_{spin}	$\cos(\theta_{spin})$
50 μrad	28.3 mrad	0.9996
100 μrad	56.7 mrad	0.9984

Goal for Spin Alignment: <50 μrad between beam direction at polarimeters and IP

- spin rotator optimization should be identical for upstream & downstream polarimeters
- monitor correlations of polarimeter measurements with local BPM trajectories;
 - + downstream polarimeter can monitor correlations with IP BPM trajectories

Impact of Crossing Angle and IR Magnets on Polarimetry

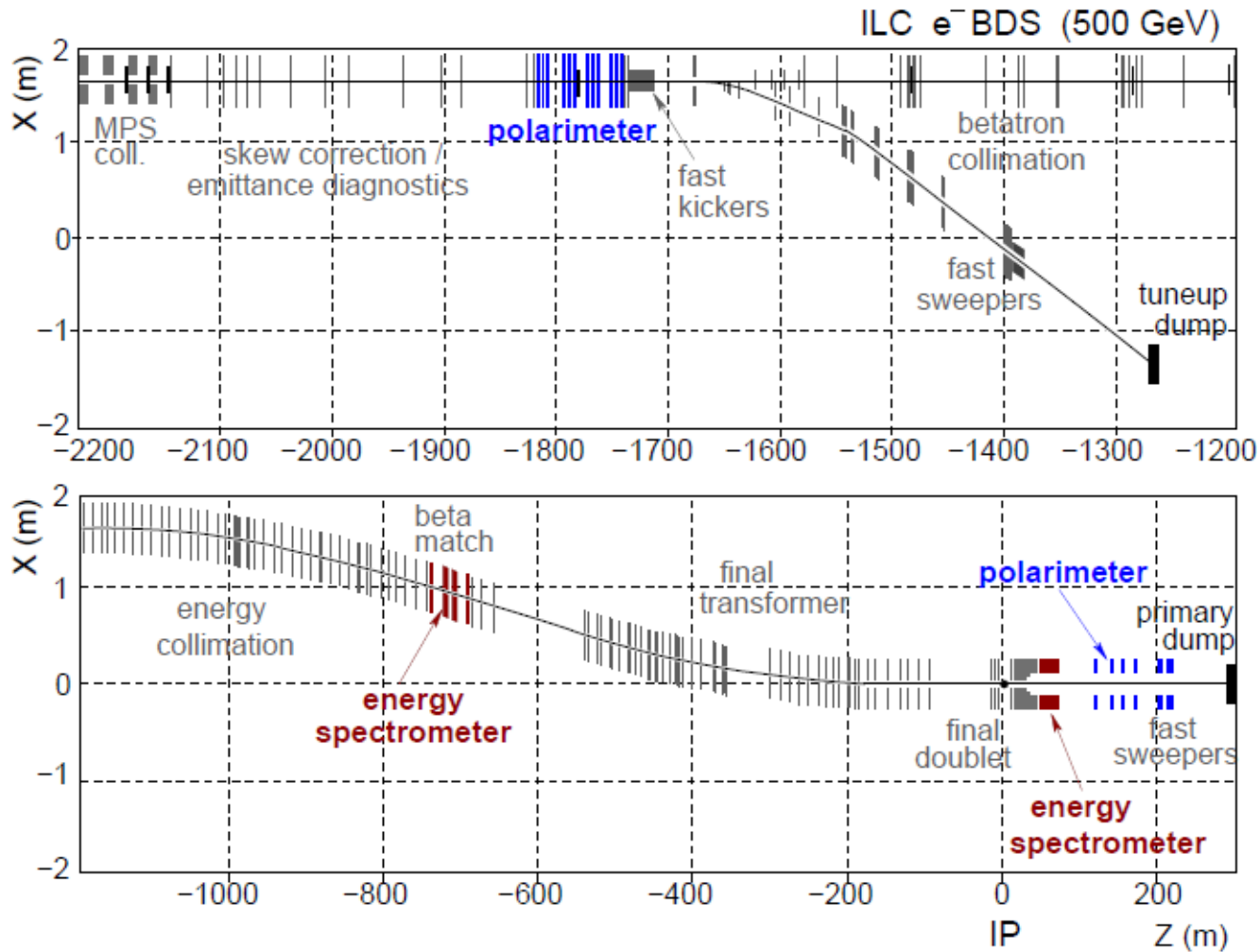
Crossing angle + Detector Solenoid has beam axis and solenoid axis misaligned. This causes a vertical deflection of the beam and affects the trajectory of low energy beamsstrahlung pairs. An "Anti-Detector-Integrated Dipole" **Anti-DID** has been designed to compensate for this. It aligns low energy pairs with the exit beampipe (good for backgrounds) but misaligns the incoming beam and the beam at the IP



Vertical trajectory of the beam in SiD with anti-DID and 14 mrad crossing angle. Collider IP is at $Z = 0$ meters.

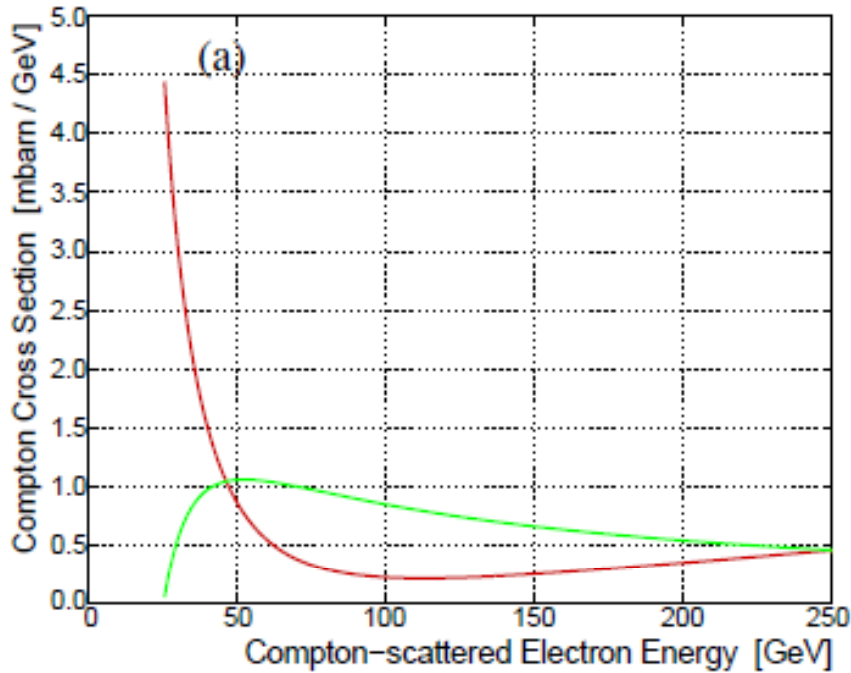
Trajectory of the beam at the upstream and downstream Compton IP s must be corrected for this vertical angle.

Polarimetry in the BDS of the ILC

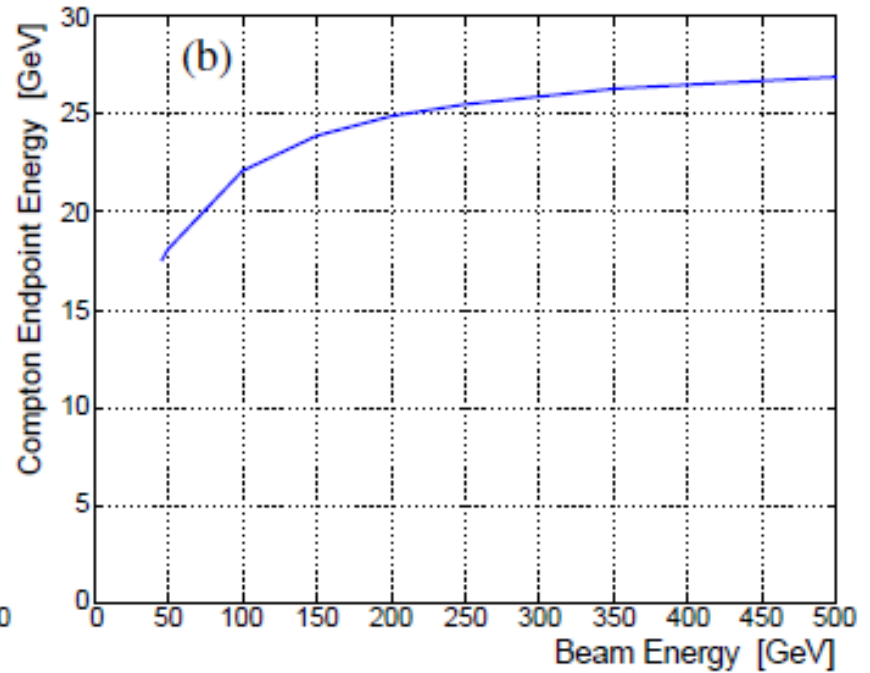


Beam Delivery System (BDS) as described in the RDR. The upper part shows the region from 2200 m to 1200 m upstream of the e^+e^- IP, including the polarimeter chicane at 1800 m. The lower part shows the region from 1200 m upstream to 400 m downstream of the IP, including the upstream energy spectrometer at 700 m as well as the extraction line energy spectrometer and polarimeter around 100 m downstream of the IP located at $z = 0$ m.

Compton differential cross section on Compton edge



(a) Compton differential cross section versus scattered electron energy for same (red curve) and opposite (green curve) helicity configuration of laser photon and beam electron.



(b) Compton edge energy dependence on beam energy.

The beam energy is 250 GeV and the laser photon energy is 2.3 eV.

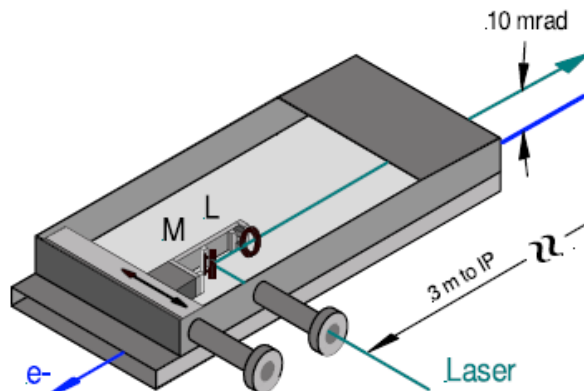
Laser

- use same laser as for TTF/Flash injector gun
- regen. multi-stage Nd:YLF amplification
[S.Schreiber et al, NIM A 445 (2000) 427]
- operates at nominal pulse & bunch pattern of TESLA
 - can hit every bunch!
- pulse length: $\sigma_t = 8$ ps
 - large fraction of laser power available for collisions
 - ~1500 scattered e^- / bunch
 - 50 W \rightarrow stat. error $< 1\%$ / s
- in routine operation for many years
- cost (in 2000): 400k Euros

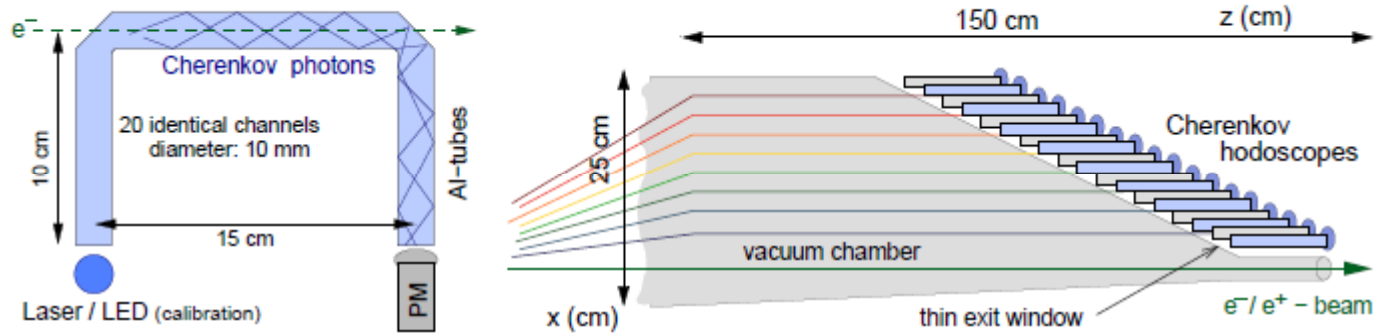


ILC Polarimetry, J. List, April 9 2008

page 8



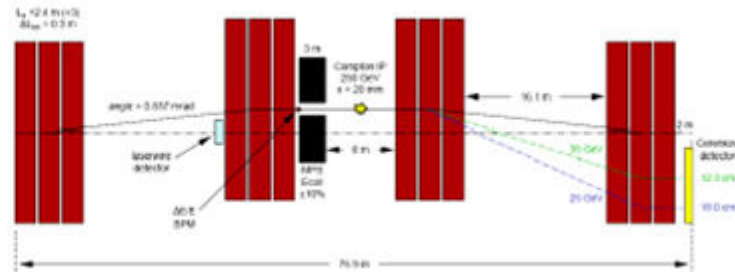
Movable mirror and lens focusing the laser onto the electron beam.



Schematic of a single gas tube (left) and the complete hodoscope array covering the tapered exit window (right) as foreseen for the Cherenkov detectors of both polarimeters.

Upstream Polarimeter: Issues

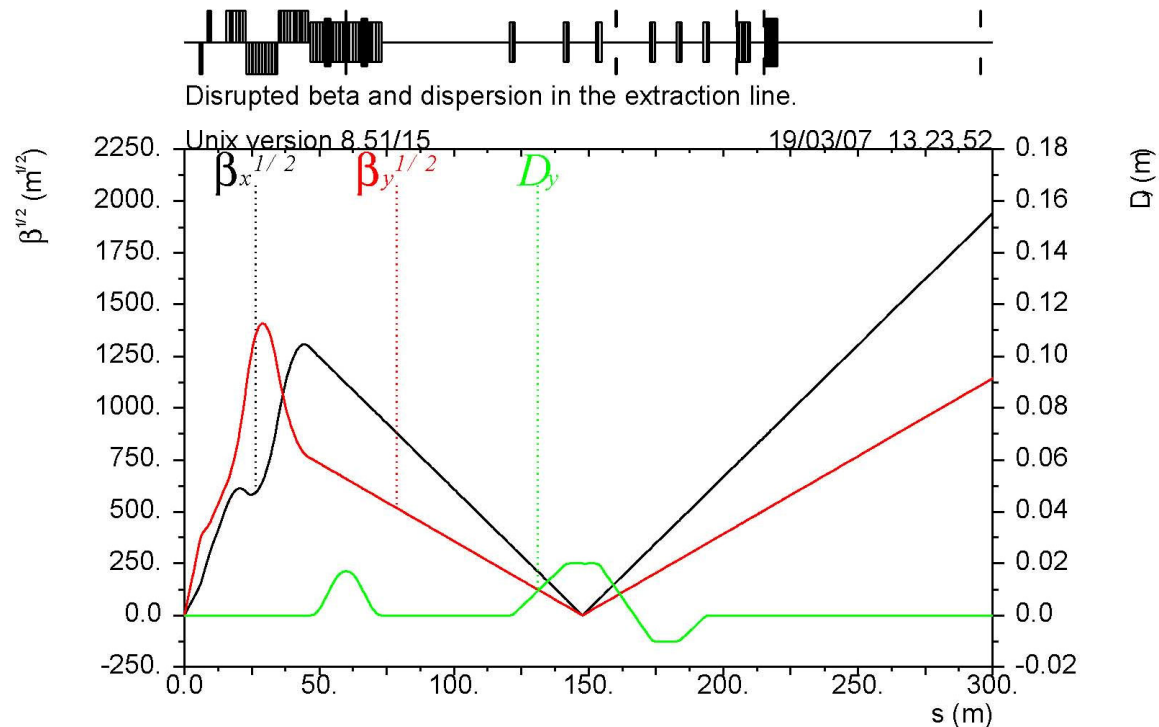
- Can the chicane host other instrumentation?
 - laser wire emittance diagnostics?
 - MPS collimator?



“The plan is to separate them but we haven't finished all work on optics yet.
Andrei Seryi

Downstream extraction line Polarimeter

Goal for Polarimeter Accuracy is $<0.25\%$



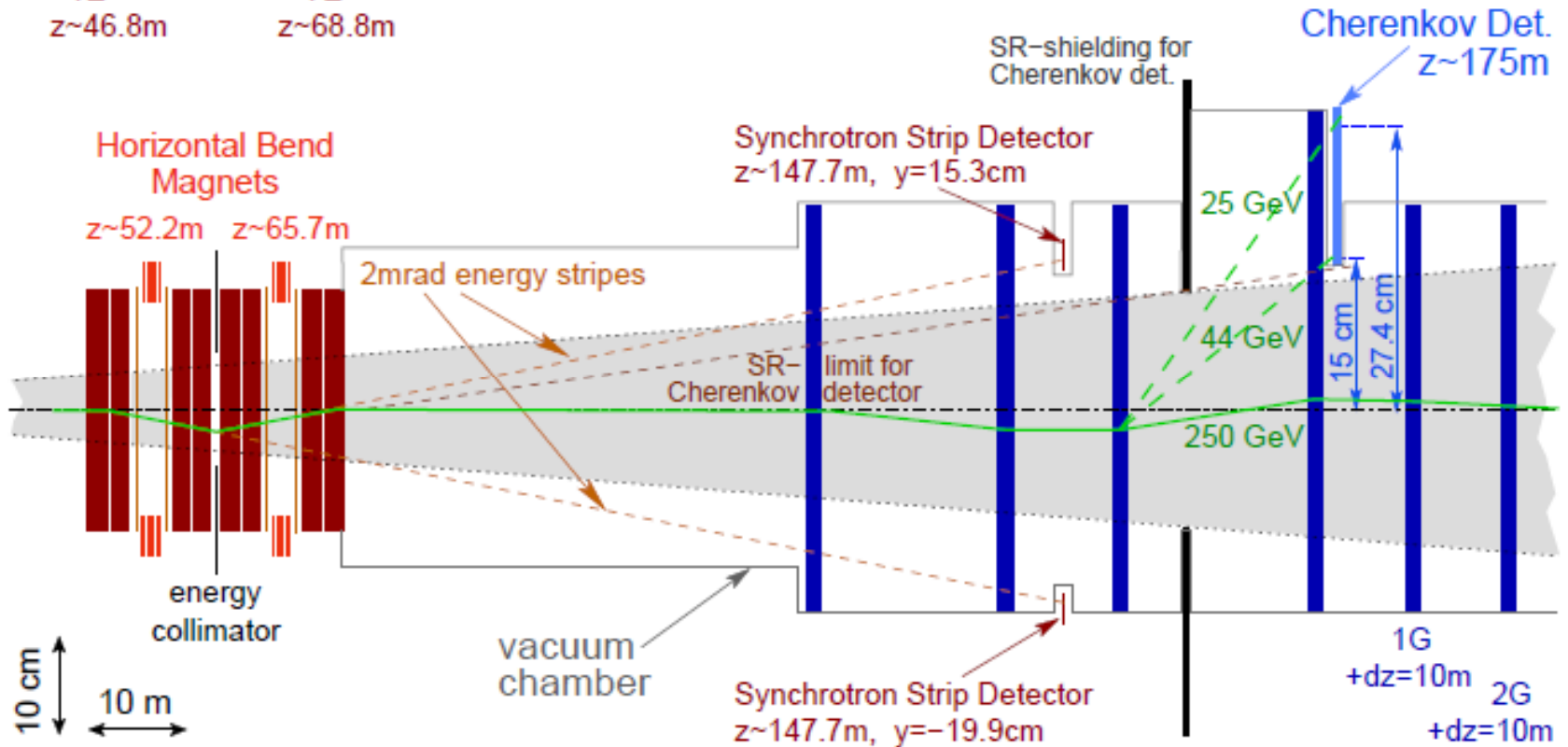
Optical β functions and vertical momentum dispersion D_y in the 14 mrad extraction line from IP to the dump, shown for the 250 GeV nominal disrupted beam.

Energy Chicane

1E z~46.8m 3E z~55.2m 7E z~68.8m

Polarimeter Chicane

1P z~120.7m 2P +dz=20m 3P +dz=12m 4P +dz=20m



Schematic of the ILC extraction line diagnostics for the energy spectrometer and the Compton polarimeter.

Laser Optics Bench

Continuum Powerlite 8000

YAG Laser

10 Hz

6ns wide

532 nm

600 mJ

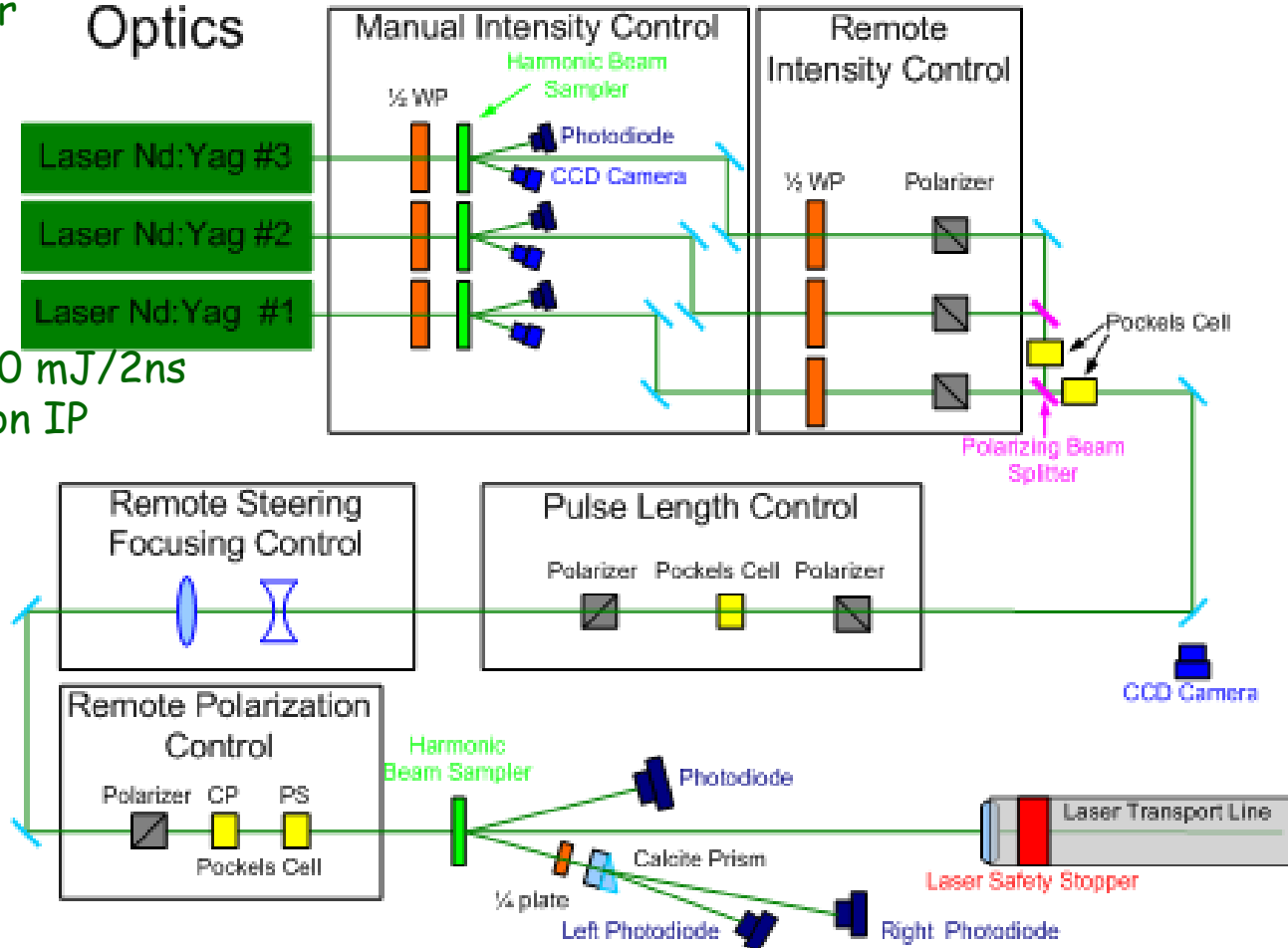
Optics

Laser Nd:Yag #3

Laser Nd:Yag #2

Laser Nd:Yag #1

Need ~100 mJ/2ns
at Compton IP



1%
measurement
every **minute**
3 bunches per
train

1%
measurement
every **hour**
180 bunches
per train

1%
measurement
every **day**
all bunches of
train

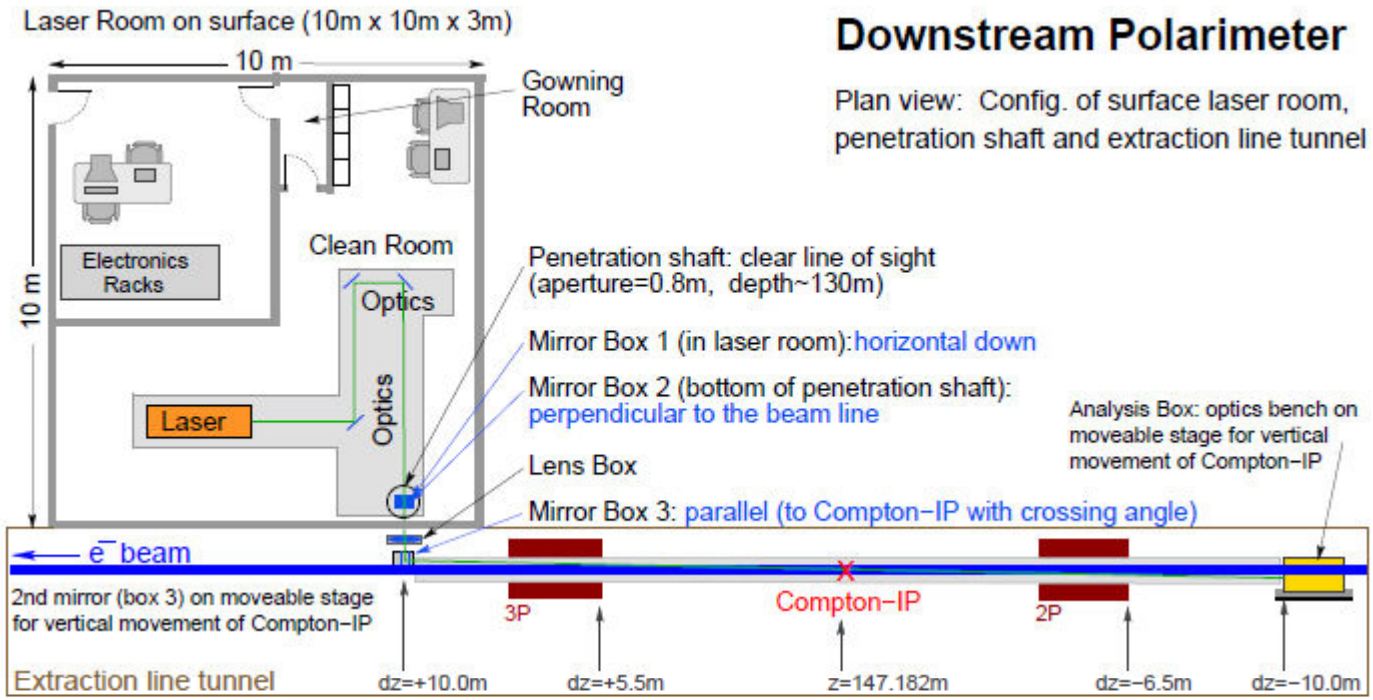
Will investigate availability of a mode-locked laser with ~35 picosec wide pulse width.

Recent new product from Quantel Pizzicato B

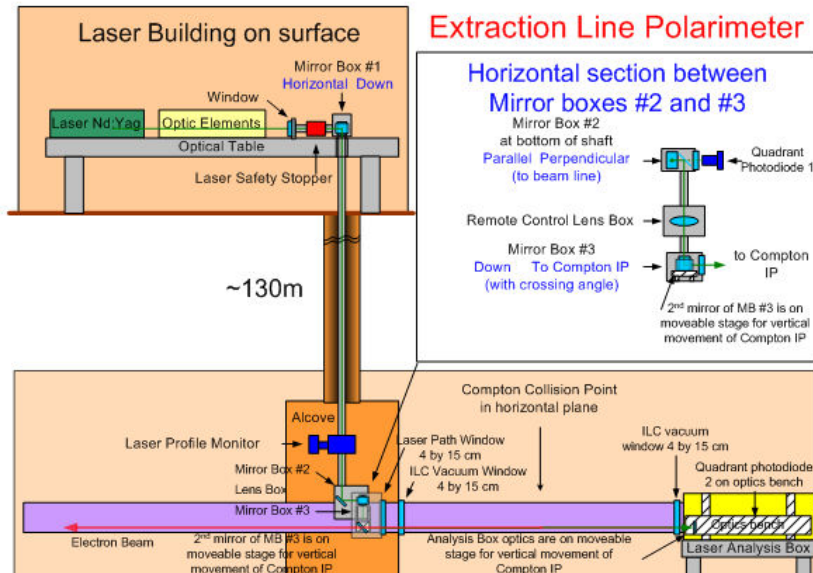
-30 mJ pulse energy at 532 nm (2.33 eV)

-20 Hz operation

-35 picoseconds

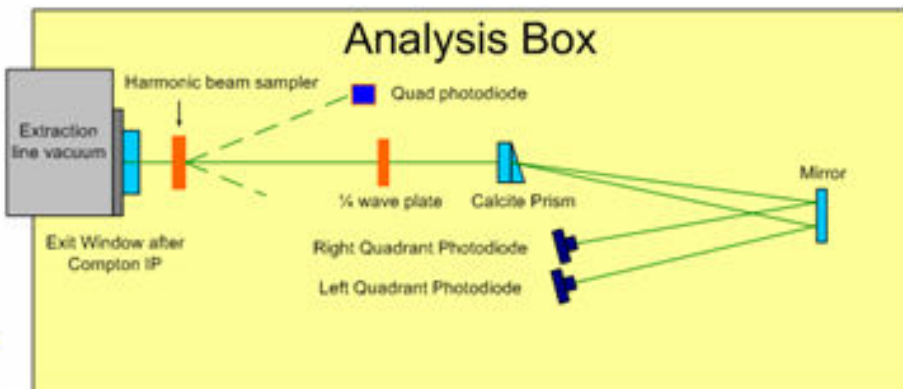
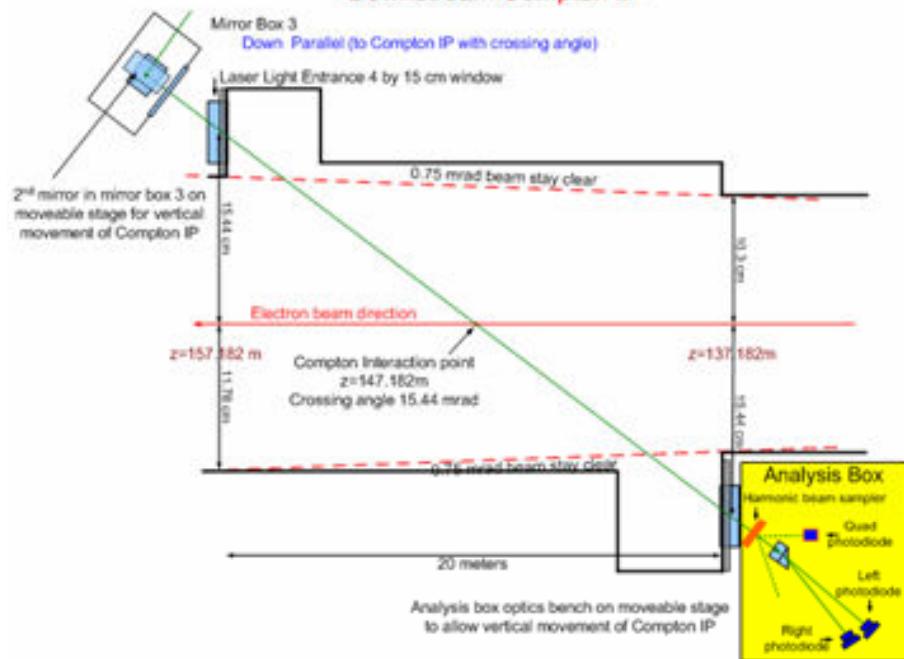


Laser Transport



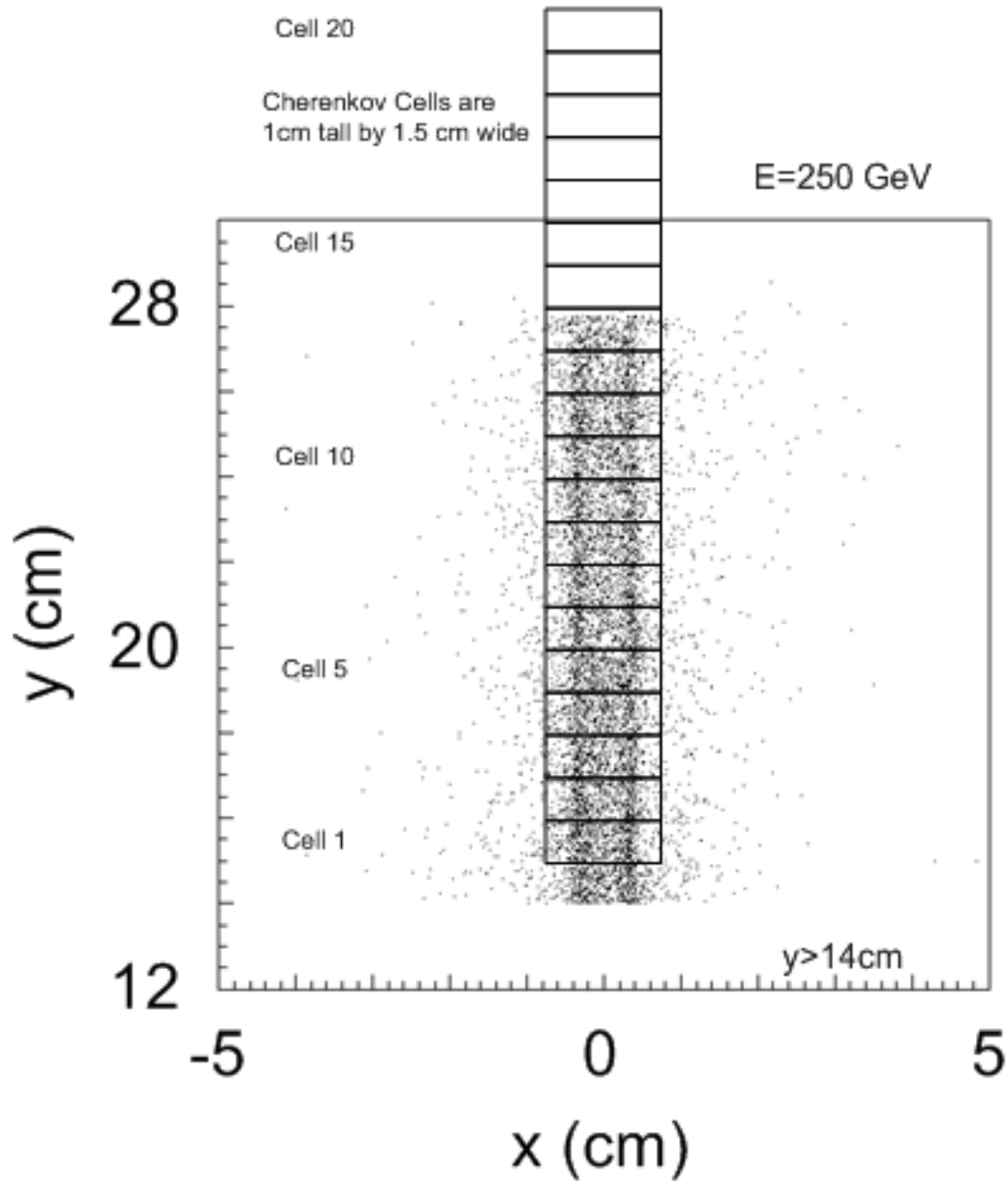
Compton IP

Downstream Compton IP

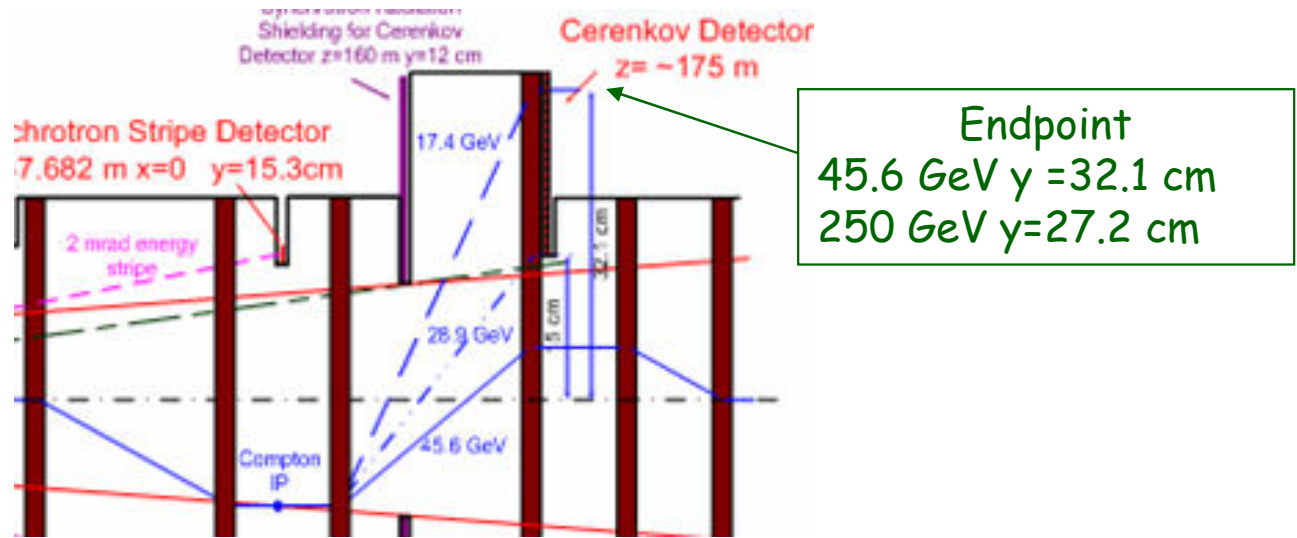


$$R^{eff} = \frac{300 \cdot \text{scattered} \cdot \text{electrons}}{\text{cm}} \cdot \left(\frac{100 \mu\text{m}}{\sigma_y} \right) \cdot \left(\frac{15.44 \text{ mrad}}{\theta_{cross}} \right) \cdot \left(\frac{E_{laser}}{100 \text{ mJ}} \right) \cdot \left(\frac{2n \text{ sec}}{t_{FWHM}} \right)$$

Compton scattered electrons at the Compton detector plane $z=175\text{m}$

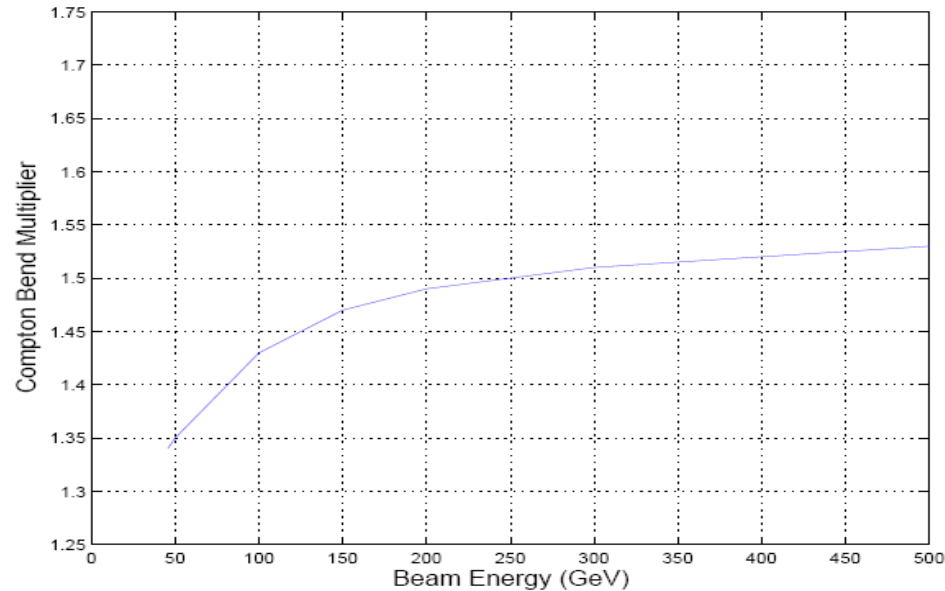
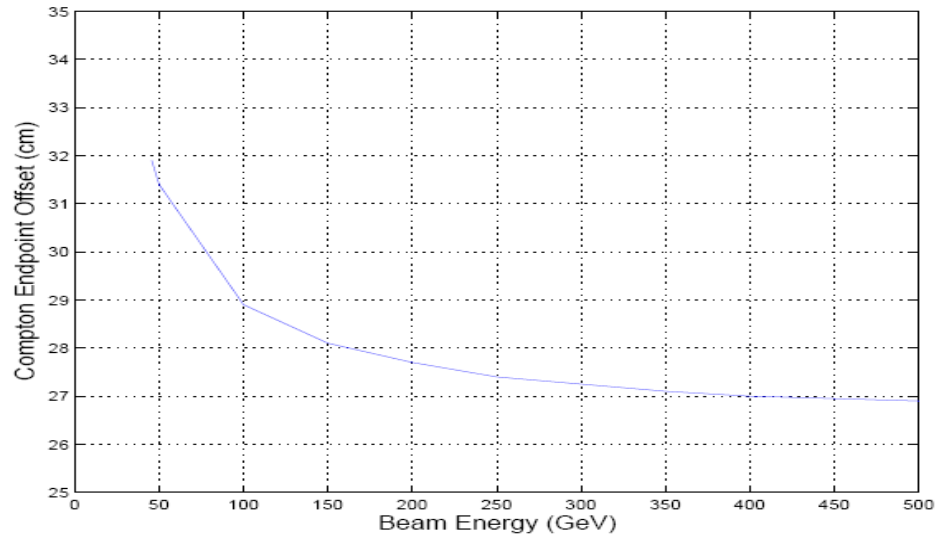


Beam Energy and Compton Endpoint



Vertical offset of the Compton endpoint for a fixed-field chicane with 20mm dispersion at 250 GeV and the last 2 polarimeter "chicane" magnets 50% stronger than the first two.

Scaling Multiplier of the last two dipoles to keep the Compton edge at 27.4cm from beamline

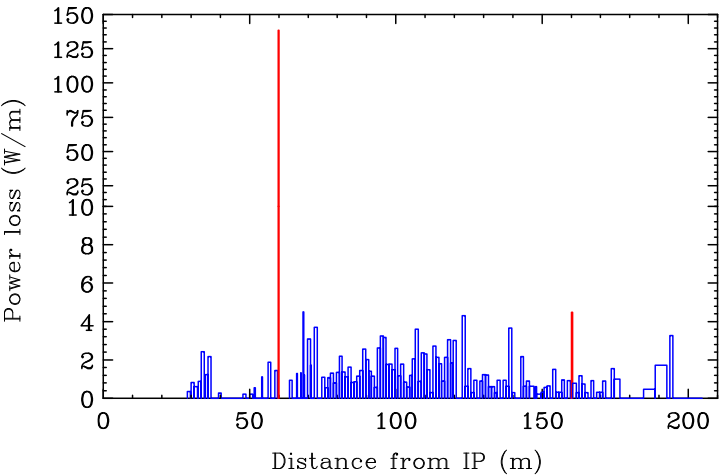


Backgrounds due to beam loss

Beam conditions for the nominal ILC parameter set show very small beam losses and no significant background is expected in the Compton electron Cherenkov detector cells.

Beam loss with worse case having large disruption: Low power option study.

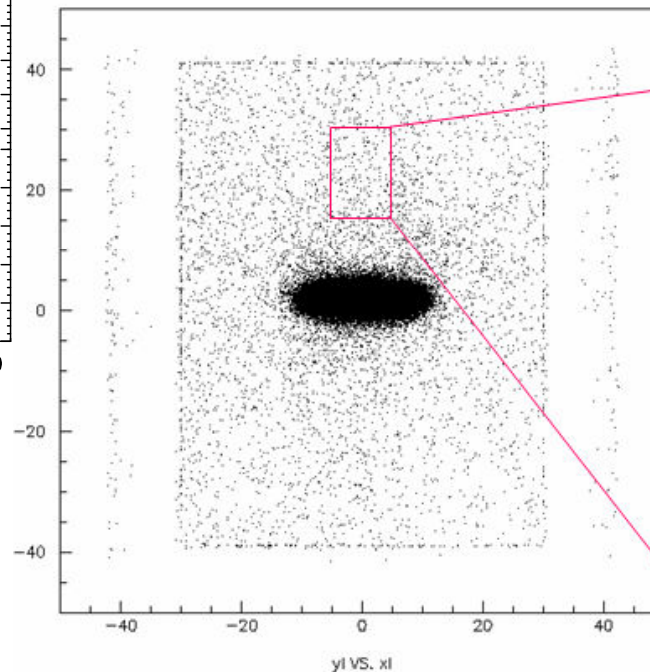
Total loss on magnets and pipe: 152 W
At chicane collimators: 42 W, 2.2 W
At dump collimators: 2.8 kW, 6.7 kW, 10.7 kW



Longitudinal density of the primary beam loss for the ILC low beam power parameter option "cs14" at 250 GeV beam energy. The two red lines show loss on the energy and polarimeter chicane collimators.

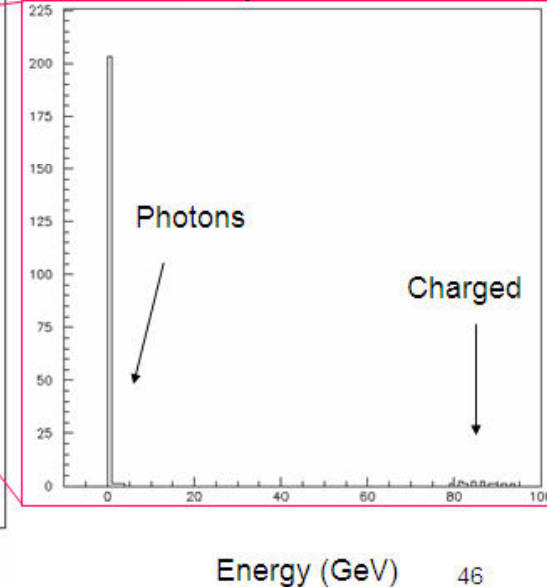
Low power option cs14 tail file with $E < 162.5$ GeV or $\theta > 0.5$ mrad

From 17.45 million beam particles



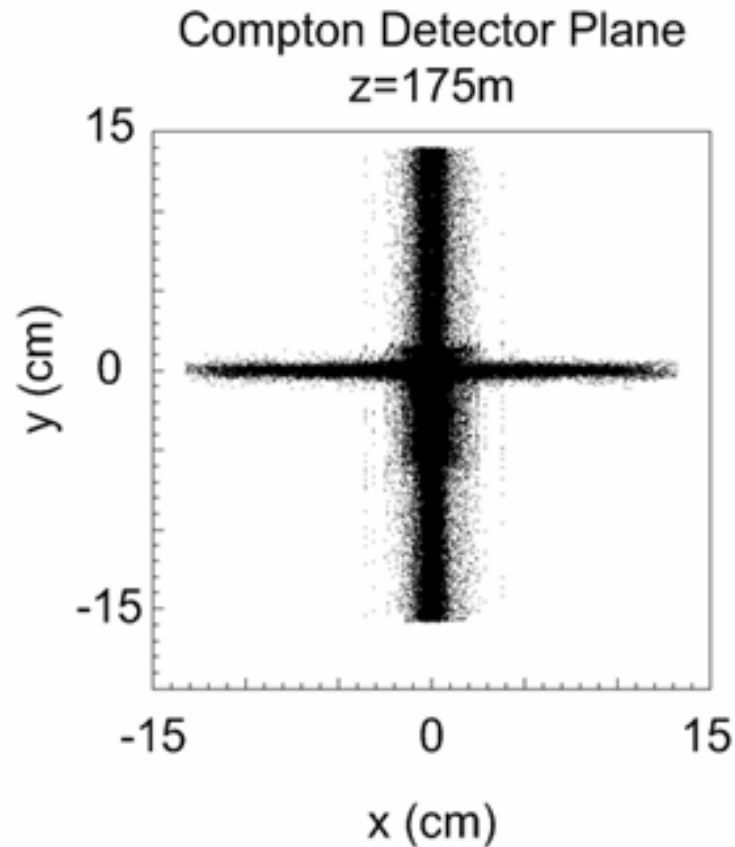
Background at the Cherenkov Detector per 2×10^{10} beam particles

92 charged / sq cm and 1558 photons / sq cm
Compared to ~300 Compton electrons per 1cm by 1.5 cm wide cell



The backgrounds from secondary interactions should be small at the Cherenkov detector compared to the signal even for the Low Power beam parameter running.

Synchrotron Radiation



Distribution of x vs y at the Compton detector plane for synchrotron radiation photons generated from the upstream magnets.

The sharp cutoff at 14 cm is the shadow from the special collimator located at $z = 160$ m.

There are no synchrotron radiation photons above 14.04 cm.

Systematic Errors

- The physics of the Compton scattering process is well understood in QED, with radiative corrections less than 0.1%
- Detector backgrounds are easy to measure and correct for by using laser off pulses;
- Polarimetry data can be taken simultaneously with physics data;
- The Compton scattering rate is high and small statistical errors can be achieved in a short amount of time (sub-1% precision in one minute is feasible);
- The laser helicity can be selected on a pulse-by-pulse basis;
- The laser polarization is readily determined with 0.1% accuracy.

Expected Polarimeter Systematic Errors

Uncertainty	dP/P
Detector Analyzing Power	0.2%
Detector Linearity	0.1%
Laser Polarization	0.1%
Electronic Noise and Background Subtraction	0.05%
TOTAL	0.25%

Measurement of the beam polarization using the W^+W^- production [1]

Ivan Marchesini ¹

Deutsches Elektronen-Synchrotron DESY, Notkestraße 85, 22607 Hamburg, Germany

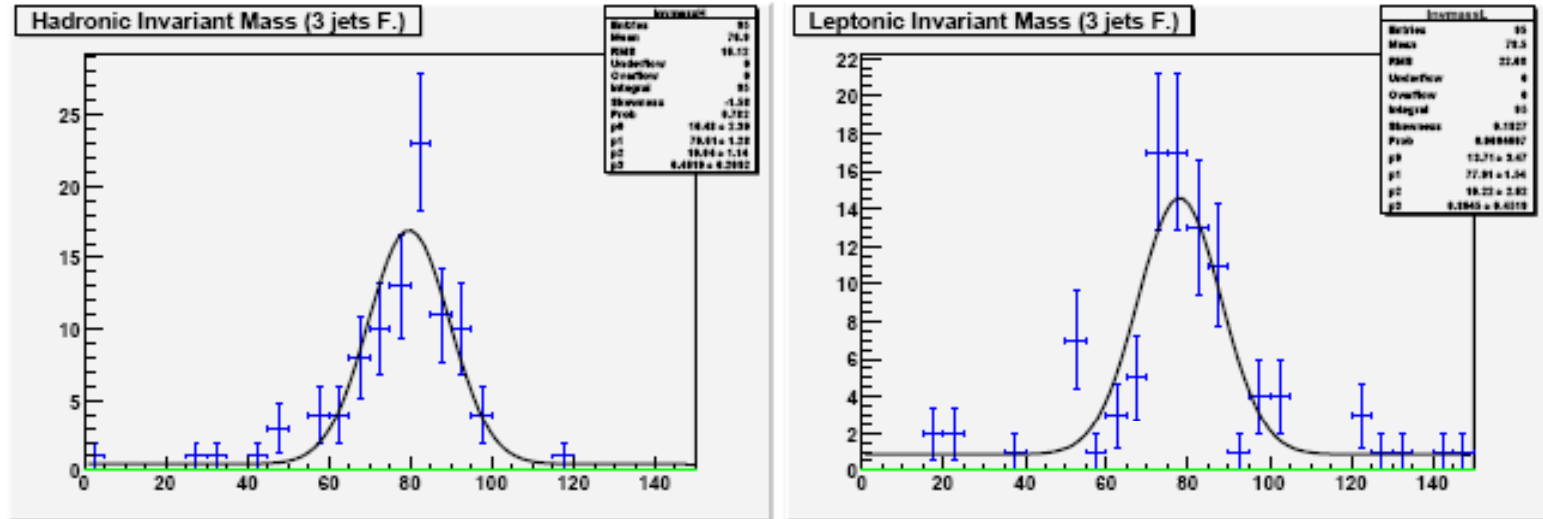


Figure 2: The W invariant mass measured from the hadronic decay (left) and from the leptonic decay (right).

The Blondel scheme

$$|P_{e^\pm}| = \sqrt{\frac{(\sigma_{-+} + \sigma_{+-} - \sigma_{--} - \sigma_{++})(\pm\sigma_{-+} \mp \sigma_{+-} + \sigma_{--} - \sigma_{++})}{(\sigma_{-+} + \sigma_{+-} + \sigma_{--} + \sigma_{++})(\pm\sigma_{-+} \mp \sigma_{+-} - \sigma_{--} + \sigma_{++})}}$$

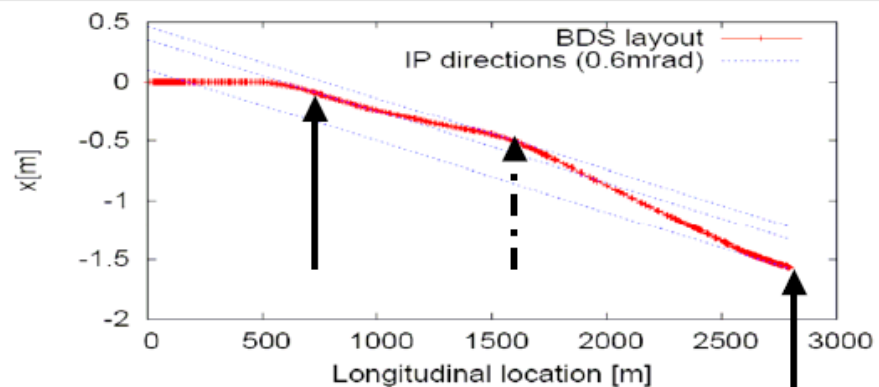
With 860 fb⁻¹ of luminosity, the error on $P_{e^-} \sim 0.1\%$ and the error on $P_{e^+} \sim 0.2\%$.

CLIC Upstream Polarimeter

Requirements: $\delta P/P = 0.25\%$

measurement robust and fast

Suitable locations



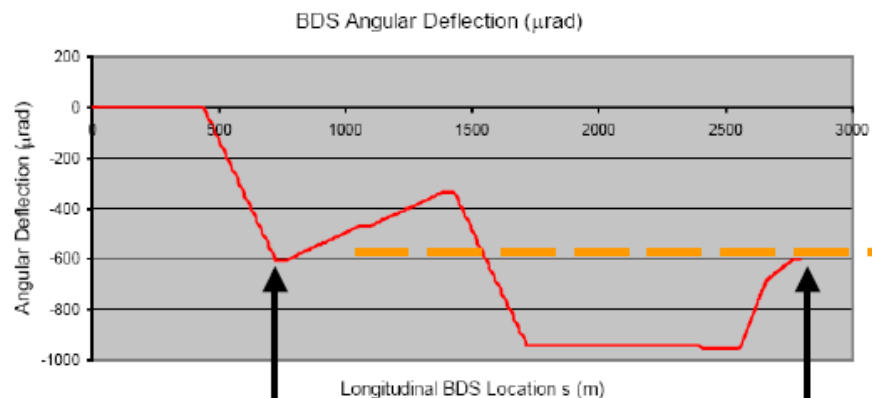
alignment exists at two locations:

$$s = 742 \text{ m}$$

$$(s = 1555 \text{ m})$$

but only the first one qualifies for polarimetry

(upstream of energy collimation and sufficient free space for laser beam crossing)



$$- 605.132 \mu\text{rad} \quad (s = 742 \text{ m})$$

$$- 601.351 \mu\text{rad} \quad (s = 2796 \text{ m})$$

aligned within $3.8 \mu\text{rad}$

Laser IP

End of BDS

CLIC Polarimeter

Orbit angle tolerances at Compton IP and IR due to spin precession considerations

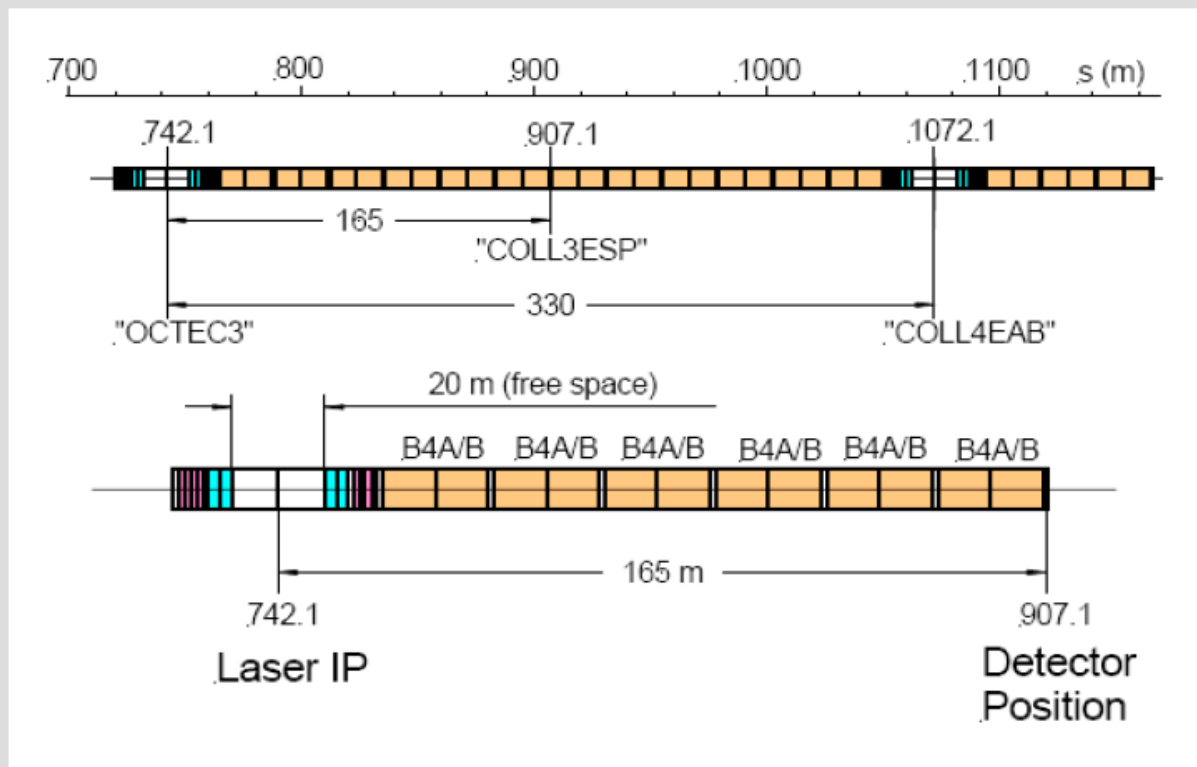
$$\theta_{spin} = \gamma \frac{g - 2}{2} \cdot \theta_{bend} = \frac{E (GeV)}{0.44065} \cdot \theta_{bend}$$
$$= 3404.06 \cdot \theta_{bend} \text{ at } 1.5 \text{ TeV}$$

Change in spin direction for various bend angles and the projection of the longitudinal polarization. Electron beam energy is 1.5 TeV.

Change in Bend Angle	Change in Spin Direction	Longitudinal Polarization Projection
100 μrad	340.4 mrad (19.5 degrees)	94.26%
50 μrad	170.2 mrad (9.75 degrees)	98.55%
25 μrad	85.1 mrad (4.87 degrees)	99.64%
13 μrad	45 mrad	99.9%

For $\delta P/P = 0.1\%$ implies angle at Compton IP and IR is aligned to better than 13 μrad .
Polarimeter needs to be before energy collimator to clean up Compton electrons.

BDS detail behind $s = 742$ m

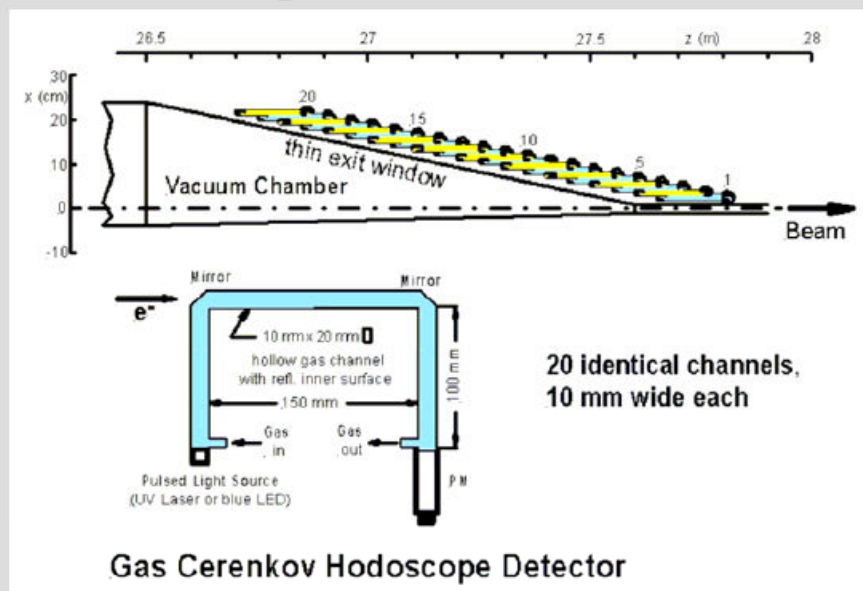


Laser IP at $s = 742$ m

Compton electron detector at $s = 907$ m

(behind 12 dipoles, as shown, or behind a lesser number of dipoles, but with reduced performance)

electron detector hodoscope



- Design similar to gas Cerenkov employed in SLD Compton polarimeter
- C_4F_{10} gas (~ 10 MeV threshold)
- detector will be immune against low-energy and diffuse background (synchr. rad.)
- could use ~ 25 channels, 10 mm wide each, to cover a large fraction of the spectrum from the Compton edge to beyond the asymmetry crossing point
- assume minimum distance of 20 mm from the beam axis
- Compton photon detection is an additional option, but will not be considered here

Conclusions

RDR Baseline:

- 30% polarized positrons
- Spin rotations systems for both electrons and positrons
 - Does not have positron helicity flip randomly pulse train to pulse train
- Upstream and downstream polarimeters for both electrons and positrons. Both upstream and downstream polarimeters required. Physics benefit of having both polarimeters justifies \$(10 to 15) million cost for either.

Positron polarization of 30% improves physics reach (factor 2 in some reactions)

Positron helicity flip important for systematic error reduction

Z-pole calibration data taking: Important to have precision measurement of polarization

ILC luminosity at Z-pole should be $\sim 8 \cdot 10^{32} \text{cm}^{-2} \text{s}^{-1}$ (40 times LEP & 400 times SLC)

Check luminosity weighted polarization measurements from upstream and downstream polarimeters, check SLD measurement and physics-based using Blondel scheme.

Calibrate upstream and downstream precision energy measurements against z-mass from LEP

Measure A_{LR} 1-day gives error on $\sin^2\theta_W$ at $\sim 10^{-4}$ (with P error of 0.25%)

Upstream Polarimeter

Decision to have a Dedicated Chicane has been reached by ILC management.

Energy collimator and laser wire system will be moved upstream of polarimeter chicane

Downstream Polarimeter

The extraction line with six magnets improves the acceptance of the Compton scattered electrons. This allows detection over a larger part of the Compton electron energy spectra.

The backscattered electrons are further away from the beam pipe by ~ 10 cm.